Acta Cryst. (1994). B50, 333–343

Incommensurately Modulated Structure of γ-PAMC: New Experimental Evidence for Amplitude and Phase Fluctuations

BY M. MEYER, W. A. PACIOREK,* K. J. SCHENK, G. CHAPUIS AND W. DEPMEIER†

Université de Lausanne, Institut de Cristallographie, BSP Dorigny, CH-1015 Lausanne, Switzerland

(*Received* 25 *September* 1993; *accepted* 18 *October* 1993)

Abstract

The incommensurate structure of γ-bis(*n*-propylammonium) tetrachloromanganate(II) (γ-PAMC) at 365 K has been determined in the superspace group *Abma*(α01)000. Main reflections and satellites up to second order have been included. Besides the harmonic model, anharmonic displacive and Debye–Waller factor modulations have been investigated. Anharmonicities of the displacive modulation functions are negligible. Global phason-correction terms significantly improve the agreement of the second-order satellites. Within the resolution of the experiment, the atomic amplitudon/phason correction converges to the expected theoretical values for the Mn and Cl atoms. The final agreement factors for a phason-corrected displacive harmonic modulation are $R_{all} = 0.052$ (1056 reflections) [$R_{main} = 0.046$ (369 reflections), $R_{1st\ order} = 0.057$ (627 reflections), $R_{2nd\ order} = 0.137$ (60 reflections)].

1. Introduction

$[NH_3C_3H_7]_2[MnCl_4]$ (PAMC) and its Cu homologue PACuC occupy a unique position within the family of the alkylammonium–metal halogenides $(C_nH_{2n+1}NH_3)_2MX_4$ due to their sequence of phase transitions (Depmeier, 1979; Doudin & Chapuis, 1990*a*) and their unique incommensurate structures [ε-PAMC, Steurer & Depmeier (1989); γ-PAMC, Depmeier (1981); γ-PACuC, Doudin & Chapuis (1990*b*), and this work]. In the general formula, $(C_nH_{2n+1}NH_3)^+$ represents a monovalent alkylammonium chain where n is up to ten or even higher, M is a bivalent metal ion ($M = Mn^{2+}$, Fe^{2+}, Cd^{2+}, Cu^{2+}) and X is a monovalent halogenide ion ($X = Cl^-$, Br^-). In these structures the ammonium ends of the organic chains are attached *via* N—H···Cl hydrogen bonds from both sides to a chessboard-like layer of corner-sharing MCl_6 octahedra. References to structural details and a review of the physical properties of PAMC can be found elsewhere (Depmeier, 1986).

At higher temperatures the so-called monoclinic hydrogen-bonding scheme (Chapuis, Kind & Arend, 1976) is thermally disordered, inducing a time-averaged symmetry higher than in the frozen state. The phase transition phenomena are connected to changes in the conformation topology.

The incommensurate phase γ of PAMC was studied by Depmeier (1981). The average structure was refined, the superspace group and a model for the modulated structure were proposed and tested in a commensurate approximation. The incommensurate phase of the Cu homologue has been recently determined (Doudin & Chapuis, 1990*b*). In this work a refinement of the incommensurate γ-PAMC is presented using the superspace group formalism, including satellites up to second order.

2. Experimental

Well suited crystals, *i.e.* free of inclusions and twinning, have been obtained at room temperature by slow evaporation of a stoichiometric aqueous solution of n-$C_3H_7NH_3Cl$ (Sigma) and $MnCl_2$ (Merck, >98%). Crystals grown on the surface of the solution were mounted directly on a glass fibre to prevent subsequent twinning. A silicone oil film (Paratone) protected the moderately hygroscopic crystals from the humidity of ambient air and delayed thermal decomposition during the experiments.

Two crystals were measured on a Syntex $P2_1$ diffractometer with Cu $K\alpha$ radiation (2θ–ω scans, graphite monochromator). For the first sample [referred to as crystal (1)], only main reflections and first-order satellites were measured up to $(\sin\theta/\lambda)_{max} = 0.37$ Å^{-1} using a U-shaped ceramic heating device (stability ±1 K); the data were used to check the superspace group reflection conditions. The second sample [referred to as crystal (2)] was heated by a dry air stream (stability ±0.3 K). In this phase the second-order satellites are very weak. Thus, at least half a sphere of main reflections and first-order

* On leave of absence from the Institute of Low Temperature and Structural Research, Polish Academy of Sciences, ul. Okólna 2, 50-950 Wrocław 2, Poland.

† Universität Kiel, Mineralogisch-Petrographisches Institut, Olsenhausenstrasse 40, D-24098 Kiel, Germany.

satellites up to $(\sin\theta/\lambda)_{max} = 0.53$ Å^{-1} were measured first. At this stage the crystal had decayed by 10%, as monitored by the standard reflections. Second-order satellites up to $(\sin\theta/\lambda)_{max} = 0.37$ Å^{-1} were subsequently measured. Due to technical difficulties, four different X-ray fluxes had to be used.

The temperature dependence of the lattice parameters, the modulation vector q and the satellite intensities were known (Depmeier, 1983). The maximum satellite intensity is found at approximately 360–370 K. In this experiment, the samples were heated at a rate of ~5–10 K min^{-1} up to the temperatures of data collection. The absolute values were estimated from the strongly temperature-dependent lattice parameter c (Depmeier, 1983): 351 (5) K and 365 (5) K from crystals (1) and (2), respectively. The lattice parameters were determined from 18 accurately centred main reflections at $2\theta \simeq 50°$ and the incommensurate component of the modulation vector, q, was found by averaging the fractional parts of index h of 10 accurately centred first-order satellites in the same 2θ range. Profiles (ω–2θ and ω scans) of main and first-order satellite reflections were measured at various diffraction angles to estimate the crystal quality. The full width at half maximum values (FWHM) were very close for main reflections and first-order satellites (see Table 1).

Three main reflections and three first-order satellites were chosen as standard reflections. Both categories exhibited identical decays during the measurement. The use of satellite reflections as standards is important for this type of experiment. Their strongly temperature-dependent intensities allow easy detection of possible instabilities in the experiment. The data reduction included scaling on all six standard reflections, an absorption correction based on the measured crystal shape and orientation, merging of equivalent reflections in accordance with the superspace symmetry and a Lorentz–polarization correction.

The data from crystal (1) confirmed the superspace group *Abma*(α01)000 [64*a*. 14.1 in de Wolff, Janssen & Janner (1981), and 64.3 in *International Tables for Crystallography* (1992, Vol. C)], as proposed by Depmeier (1981). The non-standard setting was chosen in order to ease the comparison with the other phases of this compound (Depmeier, 1981). The following reflection conditions were satisfied: $hklm$: $k + l + m = 2n$, $hk0m$: $h = 2n$, $0kl0$: $k = 2n$. For 5333 measured reflections in the 2θ range 3–70°, 45 violations of the above reflection conditions were found with $3\sigma(I) < I < 7\sigma(I)$. No effort was made to explain the forbidden intensities (*e.g.* Renninger effect, strong neighbour reflections or diffuse scattering streaks).

Table 1 summarizes the data collection conditions of crystal (2).

Table 1. *Summary of crystal and experimental data*

Crystal habit	Platelet, {001} pinacoid [0.064 (4) mm thick], {111} orthorhombic dipyramid [base: 0.618 (4) × 0.612 (4) mm]			
Space group of the average structure	*Abma* (No. 64)			
Superspace group	*Abma*(α01)000 (No. 64.3)			
Lattice parameters (Å)	a = 7.414 (2), b = 7.289 (2), c = 26.803 (7)			
V (Å^3)	1448 (1)			
Z	4			
M_r	316.98			
λ (Å)	1.54184			
D_x (Mg m^{-3})	1.462			
μ(Cu $K\alpha$) (mm^{-1})	14.01			
F(000)	652			
Modulation vector	$\mathbf{q}_1 = 0.176\,(1)\,\mathbf{a}^*$			
$hklm_{max}$	8 8 29 1 ($\|m\|$ = 0,1), 5 5 12 2 ($\|m\|$ = 2)			
$(\sin\theta/\lambda)_{max}$ (Å^{-1})	0.53 ($\|m\|$ = 0, 1), 0.37 ($\|m\|$ = 2)			
Scan width (°)	0.80 (above $K_{\alpha 1}$, below $K_{\alpha 2}$)			
Scan speed (° min^{-1})	1.04–14.65			
FWHM (°, $hklm$)	0.60 (4 0 0 0), 0.52 (0 4 0 0), 0.48 (0 0 8 0), 0.59 (0 4 13 −1), 0.52 (1 1 8 −1)			
Loss of intensity	≃30% within 216 h			
R_{int} (2θ: 3–70°, full sphere)	$\|m\|$ = 0	$\|m\|$ = 1	$\|m\|$ = 2	Total
with absorption correction	0.063	0.067	0.083	0.064
without absorption correction	0.137	0.186	0.134	0.144
Number of reflections	1846	3820	897	6563
[$> 3\sigma(I)$]	1331	2126	127	3584
Independent reflections	524	1072	292	1888
[$> 3\sigma(I)$]	369	627	60	1056
Weights	$1/\sigma^2(F)$			
Transmission factors	1.567–18.789			

3. Structure refinement

Using only Bragg intensities, three different levels of approximations can be distinguished in incommensurate structures. The average structure (valid for small modulation amplitudes) is obtained by including only main reflections to the refinement, *i.e.* neglecting all satellite intensities. The modulated structure in harmonic approximation includes harmonic atomic modulation parameters (displacive or occupational) in addition to the standard structural parameters. Finally, the highest level of approximation is reached by including anharmonic terms to the modulation functions and/or correction terms for amplitude/phase fluctuations (global or atomic). From the formal point of view, Debye–Waller factors (DWF's) can also be modulated by any harmonic (Yamamoto, 1982). A physical interpretation of this modulation has only been developed for the second harmonic terms of the DWF. These terms can be interpreted together with the standard DWF's (zero-order terms) as a parametrization of the atomic amplitude/phase fluctuations of the harmonic displacive modulation functions (see Pérez-Mato, Madariaga & Elcoro, 1991).

3.1. *Average structure*

Neglecting satellite intensities which represent, in this case, about 10% of the total scattered Bragg intensity, the average structure was refined using the

programs *SHELX* (Sheldrick, 1978) and *MSR* (Paciorek, 1991). The scattering factors for neutral atoms were taken from the *International Tables for X-ray Crystallography* (1974, Vol. IV). As starting parameters, the coordinates of the δ phase at room temperature (Peterson & Willet, 1972; adapted to the space group *Abma*) were used. In Table 2, the representative elements of the space group *Abma* are implicitly given. Table 3 lists the symmetry restrictions for atoms on special positions.

The model converged rapidly to $wR = 0.142$ with isotropic DWF's and $\sigma^{-2}(F)$ weights. Neither distance nor angle restraints were applied. Anistropic DWF's were subsequently refined for non-H atoms ($wR = 0.075$). Finally, an isotropic extinction correction was applied

$$F_{\rm calc}^{\rm corr} = F_{\rm calc}/(1 + 10^{-5} C_{\rm ext} F_{\rm calc}^2/\sin\theta)^{1/4}, \qquad (3.1)$$

where $C_{\rm ext}$ is refined in *SHELX*/*MSR*. A good agreement ($wR_{SHELX} = 0.038$, $wR_{MSR} = 0.031$) was obtained with $C_{\rm ext} = 3.1$ (3), indicating the occurrence of primary extinction.

The calculated wR factors for *SHELX* and *MSR* differ, although the refined parameters were identical in the two programs. Both use different expressions for calculating R and wR

$$R_{SHELX} = \sum|F_{i,o} - S_i F_c|/\sum F_{i,o} \qquad (3.2)$$

$$wR_{SHELX} = [\sum w(F_{i,o} - S_i F_c)^2]^{1/2}/\sum wF_{i,o}^2 \qquad (3.3)$$

$$R_{MSR} = (\sum|F_{i,o}/S_i - F_c|)/(\sum F_{i,o}/S_i) \qquad (3.4)$$

$$wR_{MSR} = [\sum w(F_{i,o}/S_i - F_c)^2]^{1/2}/\sum w(F_{i,o}/S_i)^2, \qquad (3.5)$$

where S_i is the ith scale factor, F_c the calculated structure factor and $F_{i,o}$ the observed structure factor on the ith scale.

The expressions coincide if a single scale factor is applied. Differences arise if multiple scale factors are used (four in the present case). In the current presentation, the *MSR* expressions will be used for the agreement factors.

In this refinement, the structure proposed by Peterson & Willet (1972) with the propylammonium chain on the mirror plane [position 8(f)] yielded the following bond lengths: N—C1 1.44 (2), C1—C2 1.30 (2) and C2—C3 1.56 (3) Å. Expected C—C and C—N bond lengths are: 1.54 (1) and 1.48 (1) Å, respectively (*International Tables for X-ray Crystallography*, 1968). The C1—C2 bond is shorter than expected, an effect which is frequently observed in systems with thermal vibration (Willis & Pryor, 1975). This effect has been evidenced in Raman experiments (Lucken, Hagemann & Bill, 1991). The hydrogen-bonding scheme *aab* (axial Cl2, axial Cl2, bridging Cl1; Depmeier, 1979) has latent monoclinic symmetry. Exchanges between the two mirror-related orientations result in an orthorhombic time-averaged symmetry (Chapuis *et al.*, 1976). The effect is reflected in unusually large DWF's along b if the chain is constrained on the mirror plane. Depmeier & Mason (1978) and Depmeier (1981) refined the chain on the general position 16(a) with half-population parameters to account for the orientational disorder. Following their example, a model

Table 2. *Representative elements of the superspace group Abma*(α01)000

The superspace group as generated from the above symbol contains no inversion centre that coincides with the origin. A transformation with $t = t' - \frac{1}{4}$ was therefore performed. The representative elements of the space group *Abam* can be obtained by disregarding the fourth coordinate. The superscripts enumerate the symmetry operations to identify the distances and angles given in Table 6.

Full set	(0 0 0 0) +	$(0\ \frac{1}{2}\ \frac{1}{2}\ \frac{1}{2})$ +
$^{1,9}E$	$\{x\ y\ z\ t\}$	$^{5,13}I\ \{\bar{x}\ \bar{y}\ \bar{z}\ \bar{t}\}$
$^{2,10}\sigma_x$	$\{\bar{x} + \frac{1}{2}\ y\ z + \frac{1}{2}\ \bar{t}\}$	$^{6,14}C_{2x}\ \{x + \frac{1}{2}\ \bar{y}\ \bar{z} + \frac{1}{2}\ t\}$
$^{3,11}\sigma_y$	$\{x\ \bar{y}\ z\ t\}$	$^{7,15}C_{2y}\ \{\bar{x}\ y\ \bar{z}\ \bar{t}\}$
$^{4,12}\sigma_z$	$\{x + \frac{1}{2}\ y\ \bar{z} + \frac{1}{2}\ t\}$	$^{8,16}C_{2z}\ \{\bar{x} + \frac{1}{2}\ \bar{y}\ z + \frac{1}{2}\ \bar{t}\}$

Origin on superspace group inversion centre.

Generators of the superlattice

$\{E|1,0,0,-\delta\}$ $\{E|0,\frac{1}{2},\frac{1}{2},0\}$
$\{E|0,-\frac{1}{2},\frac{1}{2},\frac{1}{2}\}$ $\{E|0,0,0,1\}$

Table 3. *Symmetry restrictions on coordinates, thermal displacement parameters and modulation parameters for the atoms on special sites*

The parentheses indicate those DWF modulation parameters which are set to zero according to the phason/amplitudon parametrization proposed by Pérez-Mato *et al.* (1991); the restrictions are calculated according to expressions (3.9) and (3.10).

Wyckoff notation 4(a); site symmetry $(\bar{1}^2)_y/(1^m)_y$; atom Mn

0	0	$x1s1$	0	$x1s2$
0	0	0	0	0
0	0	$x3s1$	0	$x3s2$
β_{11}	$(\beta_{11}c1)$	0	$\beta_{11}c2$	0
β_{22}	$(\beta_{22}c1)$	0	$(\beta_{22}c2)$	0
β_{33}	$(\beta_{33}c1)$	0	$\beta_{33}c2$	0
0	0	0	0	0
β_{13}	$(\beta_{13}c1)$	0	$\beta_{13}c2$	0
0	0	0	0	0

Wyckoff notation 8(e); site symmetry $(\bar{2}^2)_z$; atom Cl1

$\frac{1}{4}$	$x1c1$	0	0	$x1s2$
$\frac{1}{4}$	$x2c1$	0	0	$x2s2$
$x3$	0	$x3s1$	$x3c2$	0
β_{11}	0	$(\beta_{11}s1)$	$\beta_{11}c2$	0
β_{22}	0	$(\beta_{22}s1)$	$\beta_{22}c2$	0
β_{33}	0	$(\beta_{33}s1)$	$\beta_{33}c2$	0
β_{12}	0	$(\beta_{12}s1)$	$\beta_{12}c2$	0
0	$(\beta_{13}c1)$	0	0	$\beta_{13}s2$
0	$(\beta_{23}c1)$	0	0	$\beta_{23}s2$

Wyckoff notation 8(f); site symmetry $(1^m)_y$; atoms Cl2, N, C

$x1$	$x1c1$	$x1s1$	$x1c2$	$x1s2$
0	0	0	0	0
$x3$	$x3c1$	$x3s1$	$x3c2$	$x3s2$
β_{11}	$(\beta_{11}c1)$	$(\beta_{11}s1)$	$\beta_{11}c2$	$\beta_{11}s2$
β_{22}	$(\beta_{22}c1)$	$(\beta_{22}s1)$	$(\beta_{22}c2)$	$(\beta_{22}s2)$
β_{33}	$(\beta_{33}c1)$	$(\beta_{33}s1)$	$\beta_{33}c2$	$\beta_{33}s2$
0	0	0	0	0
β_{13}	$(\beta_{13}c1)$	$(\beta_{13}s1)$	$\beta_{13}c2$	$\beta_{13}s2$
0	0	0	0	0

with C1 and C2 on general positions was refined, thus yielding a significantly better agreement compared with the model of Peterson & Willet (1972). Further splittings of the remaining atoms (N, C3, Mn, Cl1 and Cl2) as presented by Depmeier (1981) did not improve the model significantly (*Tests for Statistical Significance*, *International Tables for X-ray Crystallography*, 1974). The chain was thus refined with N and C3 on the mirror plane [8(*f*)] and C1 and C2 on the general position 16(*a*) to $wR_{MSR} = 0.029$ ($\Delta_{max}/\sigma = 0.000025$ and $\Delta_{av}/\sigma = 0.00002$). Bond lengths approached close to the expected values: N—C1 1.48 (2), C1—C2 1.47 (3) and C2—C3 1.56 (3) Å.

The difference Fourier map, based on main reflections only, showed no peaks higher than ± 0.4 e Å^{-3}. The H atom positions were therefore deduced from chemical considerations and from the neutron refinement results of Depmeier & Mason (1978). Bond lengths and angles of the chain were restrained to literature values [C—H 1.04 (2), C—C 1.54 (2), N—H 1.48 (2) Å, H—C—H, H—N—H and C—C—C 109 (2)°; *International Tables for X-ray Crystallography*, 1968]; an overall isotropic Debye–Waller factor U_{iso} was applied for the H atoms. This model refined to $wR = 0.024$.

3.2. *Modulated structure from first-order satellites only*

From previous NMR investigations, the modulation is expected to be of the plane-wave type (Muralt, 1986; Muralt, Caravatti, Kind & Roos, 1986) with a maximum displacement of about 0.3 Å parallel to *c* in the *Abma* setting (Depmeier, 1983). For an atom μ, two parametrizations for the modulation function in the direction *i* are possible

$$u_i^\mu(t) = \sum_{n>0} [c_{i,n}^\mu \cos(2\pi n t) + s_{i,n}^\mu \sin(2\pi n t)] \quad (3.6)$$

$$u_i^\mu(t) = \sum_{n>0} a_{i,n}^\mu \cos[2\pi(nt + \varphi_{i,n}^\mu)], \quad (3.7)$$

with

$$t = \mathbf{q}(\mathbf{l} + \bar{\mathbf{r}}^\mu), \quad (3.8)$$

where *t* is the continuous internal coordinate ranging from 0 to 1. This expression gives the reference phase in the modulated structure of the modulation vector $\mathbf{q}$ for the atom μ in cell $\mathbf{l}$ with the basic position $\bar{\mathbf{r}}^\mu$. $c_{i,n}^\mu$, $s_{i,n}^\mu$ and $a_{i,n}^\mu$ are the amplitudes, $\varphi_{i,n}^\mu$ is the phase of the *n*th harmonic. Both expressions (3.6) and (3.7) are equivalent but (3.6) is preferred for its numerical stability. For convenience the modulation amplitudes are presented in the form (3.7).

In this refinement, two versions of the program *MSR* (Paciorek, 1991) were used: (i) a version using the analytical structure-factor expression of Paciorek & Kucharczyk (1985) for the harmonic displacive modulation and (ii) a version using the structure-factor expression proposed by de Wolff (1974) for the general case. In both versions, the refinement is based on *F* and uses the full-matrix mode. As expected, both versions gave identical results for the harmonic displacive model.

The average structure with C1 and C2 on the general position 16(*a*) was used as a starting model. The representative elements of the superspace group *Abma*(α01)000 and the symmetry restrictions for atoms on special positions are given in Tables 2 and 3. The restrictions are based on the following relations

$$\mathbf{u}^\lambda(t) = \mathbf{R}\mathbf{u}^\mu[\varepsilon^{-1}(t - \tau_4)] \quad (3.9)$$

$$\mathbf{T}^\lambda(t) = \mathbf{R}\mathbf{T}^\mu[\varepsilon^{-1}(t - \tau_4)]\mathbf{R}', \quad (3.10)$$

where μ and λ denote the properties before and after the transformation, $\mathbf{u}$ is a vector of the displacive modulation functions [expressions (3.6) or (3.7)], $\mathbf{T}$ the DWF tensor, $\mathbf{R}$ and $\mathbf{R}'$ the rotational part and its transpose of the standard space group operation, and ε and τ_4 the internal inversion and translation coordinates.

For harmonic displacive modulation the structure-factor expression of Paciorek & Kucharczyk (1985) shows that it is possible to refine the approximate amplitudes $a_{i,1}^\mu$ from the main reflections *hkl*0 only. In this procedure, the phases $\varphi_{i,1}^\mu$ have to be fixed to arbitrary values. This refinement gave approximate starting values for the amplitudes of the displacements, 0.4 Å along *c* for all atoms and 0.2–0.4 Å along *a* for Cl2 and the propylammonium chain atoms. The first-order satellites were included, allowing the refinement of the modulation phases $\varphi_{i,1}^\mu$. This model (1 in Table 4) converged rapidly to $wR_{all} = 0.038$.

3.3. *Second-order satellites*

The structure-factor expressions of Paciorek & Kucharczyk (1985) show that satellites of order ≥ 2 may originate from a harmonic displacive wave. This suggests a comparison of the harmonic with the anharmonic displacive model, including the 60 observed second-order satellites (models 2 and 3 in Table 4). Both models yielded partial agreement factors for main reflections and first-order satellites worse than model 1. Unexpectedly, the partial *R* values for second-order satellites were rather high ($wR_2 \simeq 0.19$), indicating that neither model is appropriate. This is remarkable, since the anharmonic displacive model (3) has 29 additional parameters contributing mainly to the second-order satellites.

The partial overall scaling ratio

$$\mathrm{OSR} = \Sigma F_c / \Sigma F_o \quad (3.11)$$

for second-order satellites in both models yielded

values which were systematically too high [$OSR_2(2) = 1.07$ and $OSR_2(3) = 1.10$]. A similar observation has been reported for γ-Na_2CO_3 (Holgervorst, Peterse & de Wolff, 1979), where the authors attributed this behaviour to amplitude/phase fluctuations of the modulation wave. The parametrization of these effects has been extensively discussed in the literature (Overhauser, 1971; Axe, 1980; Paciorek & Kucharczyk, 1985; Pérez-Mato *et al.*, 1991, and references therein) and continues to be controversial.

Three different parametrizations of phase/amplitude fluctuations have been applied to the harmonic displacive model: (*a*) Overhauser correction (Overhauser, 1971), model 4, (*b*) Axe correction (Axe, 1980), model 5 and (*c*) atomic phason/amplitudon correction (Pérez-Mato *et al.*, 1991), model 6.

3.4. *Overhauser correction*

This correction rescales all satellites with the following expression

$$F_c^{\rm corr} = F_c \exp(-m^2 C_{\rm Ove}), \qquad (3.12)$$

where $C_{\rm Ove}$ is the refined quantity and m is the satellite order. Overhauser (1971) derived this expression for a single-atom unit cell in terms of 'static' and 'dynamic' contributions under the assumption of global phase fluctuations, *i.e.* one overall term taking into account the possible fluctuations of the phases $\varphi^{\mu}_{i,1}$ of the atomic modulation functions.

3.5. *Axe correction*

The correction proposed by Axe (1980) postulates a global phase fluctuation of the modulation function, like in the Overhauser correction. However, the structure factor for a single-atom unit cell is evaluated in terms of 'time-average' and 'disorder' contributions, resulting in the following correction term

$$F_c^{\rm corr} = F_c \exp[-m(m-1)C_{\rm Axe}] \qquad (3.13)$$

where $C_{\rm Axe}$ is the refined quantity and m the satellite order. Both corrections rescale the satellite reflections. The Overhauser correction applies for $m \geq 1$ and the Axe correction for $m \geq 2$.

3.6. *Amplitudon/phason correction*

The amplitudon/phason correction is illustated in Fig. 1. The electron density of a hypothetical modulated structure is represented for three types of displacive modulation: (i) Static modulation – in a first approximation, the fluctuations of amplitudes and phases of the atomic modulation functions are neglected. As seen from Fig. 1, the smeared electron density of the so-called string atom shows a constant width parallel to the ordinate as a function of the internal coordinate t. The usual DWF representing the width of the smeared electron density and the atomic modulation function are sufficient to parametrize this model.

(ii) Amplitude (amplitudon) and (iii) phase fluctuations (phason) of the atomic modulation functions – in the general case, the atomic modulation functions are dynamic and may fluctuate in amplitude and phase. The magnitude of the fluctuations is determined by a structure-specific parameter $\langle\delta\varphi^2\rangle - \langle\delta\rho^2\rangle$ explained below. This term influences all the individual DWF's. In this model, the electron density varies in width as a function of the internal coordinate t (see Fig. 1). The DWF expressing the width of the smeared electron density has to be modulated.

Pérez-Mato *et al.* (1991) derived a modulated DWF for the general case of mixed amplitude and phase fluctuations of a harmonic atomic modulation function. This parametrization will be called APC (amplitudon/phason correction) hereafter. Expressed with β the modulated DWF takes the following form [the expressions (3.14)–(3.18) are taken from Madariaga, Pérez-Mato & Aramburu (1993)]

$$\beta^{\mu}_{ij}(t) = \beta^{\mu}_{ij,0} + \beta^{\mu}_{ij,2}\cos(4\pi t + \chi^{\mu}_{ij,2}). \qquad (3.14)$$

This expression contains two parts: $\beta^{\mu}_{ij,0}$ is constant and independent of the internal coordinate t and satisfies the relation

$$\beta^{\mu}_{ij,0} = \beta^{\mu}_{ij,h} + \beta^{\mu(0)}_{ij,2}\cos(\varphi^{\mu}_{i,1} + \varphi^{\mu}_{j,1}) \qquad (3.15)$$

with

$$\beta^{\mu(0)}_{ij,2} = \pi^2 a^{\mu}_{i,1} a^{\mu}_{j,1}[\langle\delta\varphi^2\rangle + \langle\delta\rho^2\rangle], \qquad (3.16)$$

where $\beta^{\mu}_{ij,h}$ is the DWF term due to the excitations of the basic periodic structure and $\beta^{\mu(0)}_{ij,2}$ the term due to amplitude and phase fluctuations of the atomic modulation function in the directions i and j. Their amplitudes ($a^{\mu}_{i,1}$ and $a^{\mu}_{j,1}$) and phases ($\varphi^{\mu}_{i,1}$ and $\varphi^{\mu}_{j,1}$) are given in the form of expression (3.7). $\langle\delta\varphi^2\rangle$ and

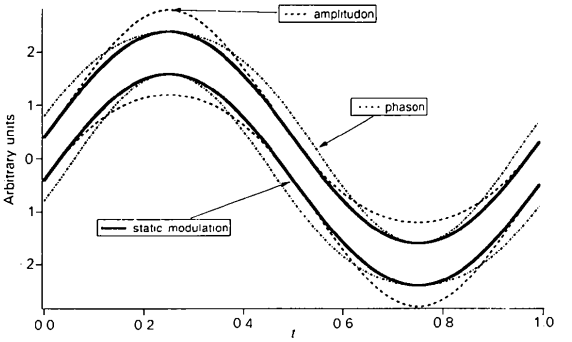

Fig. 1. Schematic representation of the effect of second-harmonic Debye–Waller factor modulation [parametrization after Pérez-Mato *et al.* (1991) and representation modified after de Wolff (1974)]. See text for expression (3.6).

Table 4. *R factors for the modulated structure (various models)*

Model 1, harmonic displacive, only satellites with $|m| = 1$; 2, harmonic displacive; 3, anharmonic displacive; 4, harmonic displacive, Overhauser correction (global phason); 5*a*, harmonic displacive, Axe correction (global phason), $I > 3\sigma(I)$; 5*b*, harmonic displacive, Axe correction (global phason), all observed reflections; 6, harmonic displacive, second harmonic for DWF's (atomic phason/amplitudon); 7, harmonic displacive, first harmonic for DWF's; 8, harmonic displacive, H atoms included, Axe correction (global phason). For all models: $\Delta_{max}/\sigma < 0.001$, the goodness-of-fit $\simeq 2$, $OSR_{all} \simeq 0.99$, weights $= 1/\sigma^2(F)$, R values are multiplied by 100. Expressions: R_{all} (3.4); wR (3.5); OSR (3.11); N_p, number of parameters.

Model	R_{all}	wR_{all}	wR_{main}	wR_{sat}	wR_1	wR_2	OSR_2	N_p	$C^{Axe/Ove}$
1	5.07	3.82	3.1	6.5	6.5	-	-	79	-
2	5.59	4.66	3.5	8.2	7.1	19.5	1.07	79	-
3	5.46	4.48	3.4	7.7	6.7	18.1	1.10	108	-
4	4.98	3.89	3.1	6.7	6.4	12.1	0.93	80	0.13 (1)
5*a*	5.22	3.93	3.1	6.8	6.5	11.9	0.91	80	0.17 (1)
5*b*	9.81	6.82	6.2	9.1	6.6	18.9	0.72	80	0.17 (1)
6	4.89	3.67	2.9	6.3	6.0	11.1	0.93	130	-
7	5.18	4.27	3.4	7.0	5.9	18.4	1.06	137	-
8	5.30	4.11	2.9	7.8	6.8	18.8	1.07	102	-

$\langle\delta\rho^2\rangle$ are the mean-square phase and amplitude fluctuations, respectively.

The second part $\beta^{\mu}_{ij,2}\cos(4\pi t + \chi^{\mu}_{ij,2})$ accounts for the fluctuations depending on the internal coordinate t. $\beta^{\mu}_{ij,2}$ is given as

$$\beta^{\mu}_{ij,2} = \pi^2 a^{\mu}_{i,1} a^{\mu}_{j,1}[\langle\delta\varphi^2\rangle - \langle\delta\rho^2\rangle], \qquad (3.17)$$

which contains the same terms as in (3.16). The phase $\chi^{\mu}_{ij,2}$ of the modulated DWF is determined by the phases $\varphi^{\mu}_{i,1}$ and $\varphi^{\mu}_{j,1}$ of the harmonic modulation wave in the directions i and j

$$\chi^{\mu}_{ij,2} = \varphi^{\mu}_{i,1} + \varphi^{\mu}_{j,1} + \pi. \qquad (3.18)$$

It is thus possible to check the APC parametrization of Pérez-Mato *et al.* (1991) by comparing the refined phases $\varphi^{\mu}_{i,1}$ and $\varphi^{\mu}_{j,1}$ of the atomic modulation function with $\chi^{\mu}_{ij,2}$.

The site symmetry induces restrictions on the positional, DWF and modulation parameters for atoms on special positions [see Table 3 and expressions (3.9) and (3.10)]. Considering expression (3.15), further restrictions may arise for the APC, because $\beta^{\mu}_{ij,2}$ is zero if one or both of the displacive modulation amplitudes in the directions i and j are zero. These additional restrictions are presented in Table 3 as well.

The three models 4, 5 and 6, corrected for the phase/amplitude fluctuations, improved the agreement when compared with model 2. The final R values are presented in Table 4. Note that their OSR_2 values are smaller than 1.0 and that their partial R values for main reflections and first-order satellites are comparable to the corresponding values of model 1.

From the formal point of view, the DWF's can be modulated using the first harmonic (Yamamoto, 1982). No physical justification of this procedure has been given up to now. This parametrization is included here for the sake of completeness in model 7 (Table 4).

3.7. H *atoms in the modulated structure*

H atoms have been tentatively included in the harmonic displacive model starting from the coordinates of the average structure (model 8 in Table 4). The modulation parameters of the H atoms were approximately constrained to the values of the adjacent chain atoms. [An exact coupled movement of the chain atoms and their H atoms can only be simulated if the reference phase of the constrained H atoms is $\mathbf{q}\cdot\mathbf{r}_{chain}$, see expression (3.8), and not $\mathbf{q}\cdot\mathbf{r}_H$ as supported by MSR.] This approximation is justified since $x_{chain} \simeq x_H$. Restraints on distances and angles were applied as in the average structure.

4. Results and discussion

4.1. *Displacive modulation*

The refined average structure agrees well with the result of Depmeier (1981) for γ-PAMC at 360 K. The coordinates correspond to the medium positions of the previous study with various split atoms. Higher DWF's for the Mn and Cl atoms can be attributed to a lower resolution [$(\sin\theta/\lambda)_{max} = 0.53$ Å^{-1} *versus* 0.71 Å^{-1} Depmeier, 1981).

The structure of PAMC consists of two-dimensional layers of corner-sharing $MnCl_6$ octahedra to which propylammonium chains are attached from both sides *via* N—H···Cl hydrogen bonds. These structural units are stacked on top of each other. Van der Waals forces between methyl groups hold the neighbouring layers together.

In Table 5* the parameters of the harmonic displacive model with Axe correction (model 5) are presented. The errors are calculated according to Rollet (1965). The positional parameters of the average and the basic structure are practically identical. Fig. 2 illustrates how enlarged DWF's partially cover the effect of a displacive modulation with small amplitude.

The harmonic displacive modulation has its dominant amplitudes in the *ac* plane. Along *a*, the amplitudes are important for the chain atoms and Cl2 and range from 0.122 (8) to 0.49 (2) Å. Along *c*,

* A list of the structure factors of model 5 have been deposited with the British Library Document Supply Centre as Supplementary Publication No. SUP 71638 (5 pp.). Copies may be obtained through The Technical Editor, International Union of Crystallography, 5 Abbey Square, Chester CH1 2HU, England. [CIF reference: DU0377]

Table 5. *Refined parameters of model 5*

The positional coordinates of the average and modulated structure coincide. The DWF's are refined as β_{ij}^{*}. U_{ij} of the modulated and the average structure are given for comparison. The coordinates (x, y, z) and modulation amplitudes (a_x, a_y, a_z) are multiplied by 10^4, the DWF's by 10^3 and the modulation phases (φ_x, φ_y, φ_z) are given as multiples of 2π.

Isotropic exinction 2.6 (2), formula (1), Axe parameter 0.17 (1), formula (5)

	x a_x φ_x	y a_y φ_y	z a_z φ_z	β_{11} U_{11} $U_{11,av}$	β_{22} U_{22} $U_{22,av}$	β_{33} U_{33} $U_{33,av}$	β_{12} U_{12} $U_{12,av}$	β_{13} U_{13} $U_{13,av}$	β_{23} U_{23} $U_{23,av}$	U_{eq} $U_{eq,av}$
Mn	0*	0*	0*	12.2 (4)	12.5 (4)	2.46 (4)	–	−0.10 (6)	–	
	8 (2)	–	139.5 (8)	34 (1)	34 (1)	9.0 (1)	–	−1.0 (1)	–	5.3
	0.25*	–	0.75*	35 (2)	35 (2)	17.9 (3)	–	−3.6 (9)	–	8.3
Cl1	7500*	7500*	5087.0 (5)	14.5 (4)	15.0 (4)	3.19 (4)	3.4 (2)	–	–	
	13 (2)	3 (3)	136.1 (8)	40 (1)	40 (1)	11.6 (2)	9 (5)	–		6.5
	0.00*	0.50*	0.25*	41 (2)	42 (2)	20.3 (3)	9 (5)	–	–	9.5
Cl2	419 (3)	0*	910 (1)	20.8 (4)	30.0 (5)	2.53 (4)	–	−0.08 (8)	–	
	174 (2)	–	137.9 (9)	58 (1)	81 (1)	92 (1)	–	−0.07 (7)		7.7
	0.520 (2)	–	0.750 (1)	69 (2)	82 (2)	185 (3)	–	−3 (1)	–	11.2
N	−240 (10)	0*	4169 (4)	28 (1)	30 (1)	2.1 (1)	–	0 (3)	–	
	164 (8)	–	122 (2)	79 (3)	80 (4)	75 (4)	–	0 (3)		7.8
	0.450 (7)	–	0.254 (4)	90 (5)	83 (5)	132 (8)	–	7 (5)	–	10.2
C1	720 (20)	400 (30)	3699 (6)	53 (3)	24 (5)	3.2 (2)	3 (3)	−1 (1)	−0.001 (1)	
	240 (10)	50 (20)	108 (5)	147 (8)	60 (10)	118 (8)	9 (9)	−10 (10)	−0.01 (1)	10.8
	0.528 (9)	0.37 (7)	0.268 (8)	170 (10)	70 (20)	190 (20)	0.01 (1)	−20 (10)	−0.02 (1)	14.4
C2	−190 (30)	−490 (30)	3272 (7)	105 (5)	32 (5)	3.2 (3)	−18 (4)	2 (1)	−0.0005 (8)	
	560 (20)	100 (200)	124 (5)	290 (20)	90 (10)	120 (10)	−50 (10)	20 (10)	−0.005 (7)	16.7
	0.553 (6)	0.74 (4)	0.258 (8)	290 (30)	90 (20)	190 (20)	−40 (20)	20 (10)	−0.01 (2)	19.0
C3	940 (30)	0*	2800 (5)	93 (4)	86 (5)	3.0 (2)	-	4.0 (8)	–	
	660 (20)	–	132 (5)	260 (10)	230 (10)	108 (8)	-	4.0 (8)	–	19.9
	0.561 (5)	–	0.241 (7)	360 (30)	240 (20)	220 (20)	–	10 (20)	–	27.0

all atoms show modulations ranging from 0.29 (1) to 0.374 (1) Å. Owing to their site symmetry, additional modulations along b are possible for Cl1, C1 and C2. None exceed 0.07 (1) Å. These modulations may therefore be considered as plane-wave type in accordance with the results obtained from NMR (Muralt, 1986).

In the harmonic model, the modulation phases of the dominant amplitudes are all in phase (Fig. 3). This can be interpreted as a cooperative movement of the octahedra and the chains. This behaviour is also reflected in the bond length variations as a function of t. Within the octahedron, the bond lengths vary by 0.01 Å [Table 6, (I)], and by 0.03–0.08 Å within the chain [Table 6, (II)]. The positional uncertainty as estimated from the DWF's is approximately 0.2–0.5 Å. It can be concluded that the octahedra and the chains are essentially rigid in the structure. Both are linked by rigid N—H···Cl hydrogen bonds as reflected by the neglegible variation in the N···Cl contact length [Table 6, (III)]. The modulation thus affects the whole ensemble.

The distances between the terminal methyl groups of adjacent layers show a wider variation than the distances affecting the octahedron and the chain: 0.21 (4)–0.26 (2) Å [Table 6, (IV)]. This can be viewed in the context of the origin of the incommensurate phase as proposed by Muralt (1986): This author ascribes the apparition of the incommensurate phase to the coupling of the interlayer methyl distance with the tilting angle of the organic N—C1 bond as observed by NMR. From his measurements, an angle of 4° was deduced for the modulation amplitude, which agrees with the value of 4 (2)° in this analysis. The high standard deviation originates in the error contribution of several atomic modulation functions.

A number of tests were performed to check the occurence of systematic errors in the data set: normal probability plot (*International Tables for X-ray Crystallography*, 1974), F_c *vs* F_o, $(F_o - F_c)/F_o$ *vs* F_o, $\sin\theta/\lambda$, reflection number. The first two are shown in Fig. 4. No anomalous behaviour can be detected.

4.2. *Second-order satellites: Overhauser, Axe correction and amplitudon/phason correction*

Based on the refinement of model 1, additional models have been tested including the 60 second-order satellites. Without phason correction, the harmonic (2), anharmonic (3) or first-harmonic DWF modulation (7) models yielded unsatisfactory results for all reflection categories. This is mainly due to the incapability of these models to accommodate main reflections and first-order with the second-order satellites. Only models including an overall or atomic phason correction (APC) yielded satisfactory results (models 4, 5 and 6).

Table 6. *Bond lengths and angles* (Å, °)

Bond distances and angles of model 5. The superscript in front of the atom identifier refers to the symmetry operations in Table 2; d_{av} average distance (Å); a_{av} average angle (°); for d_{av} and a_{av}, the average standard deviations are given in parentheses; d/a_{min} minimal distance/angle; d/a_{max} maximum distance/angle; Δ difference between max and min.

	d/a_{av}	d/a_{min}	d/a_{max}	Δ
(I) Octahedron				
Mn—^{11}Cl1	2.610 (1)	2.606	2.614	0.008
Mn—^{6}Cl1	2.610 (1)	2.606	2.614	0.008
Mn—^{9}Cl1	2.610 (1)	2.606	2.614	0.008
Mn—Cl2	2.460 (3)	2.457	2.463	0.006
^{6}Cl1—Mn—Cl2	89.92 (7)	89.86	89.98	0.12
^{6}Cl1—Mn—^{9}Cl1	91.46 (4)	91.33	91.68	0.35
^{11}Cl1—Mn—^{9}Cl1	88.53 (4)	88.24	88.82	0.58
^{6}Cl1—Mn—^{11}Cl1	179.0 (2)	179.0	179.0	0.9
(II) Chain				
N—C1	1.48 (2)	1.47	1.50	0.03
C1—C2	1.45 (3)	1.39	1.52	0.13
C2—C3	1.52 (3)	1.47	1.58	0.11
N—C1—C2	113 (2)	109	118	9
C1—C2—C3	109 (2)	102	117	15
(III) Hydrogen bonds				
^{15}N—Cl2	3.6537 (7)	3.6520	3.6556	0.0036
^{15}N—^{16}Cl2	3.226 (8)	3.217	3.236	0.019
^{15}N—^{9}Cl1	3.378 (7)	3.363	3.391	0.028
(IV) Interlayer C3—C3 distances [corresponding to those given in Doudin & Chapuis (1990*a*) and Doudin & Chapuis (1990*b*) for the Cu homologue of PAMC]				
^{16}C3—^{6}C3	4.20 (1)	4.11	4.37	0.26
^{16}C3—C3	4.41 (2)	4.31	4.52	0.21
^{16}C3—^{13}C3	4.07 (3)	3.93	4.16	0.23

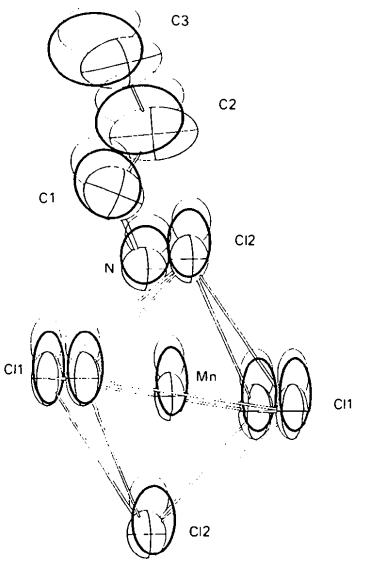

Fig. 2. *ORTEP* (Johnson, 1965) plot showing a projection abong *b* of one octahedron and one corresponding propylammonium chain. The heavy lines show the outline of the Debye–Waller factors of the average structure, the fine lines show the basic structure for two extreme modulation displacements ($t \simeq 2/6$ and 4/6).

In order to evaluate the impact of the phason corrections on the models, the structure-factor expressions of a single-atom structure will be discussed for a harmonic and an APC corrected model. The following structure-factor expressions are derived for the reflections (00*lm*) using the results of Paciorek & Kucharczyk (1985), Pérez-Mato *et al.* (1991) and Paciorek & Chapuis (1994): (*a*) harmonic displacive modulation

$$|F^{stat}_{00lm}| = T^{stat}A^{stat} = \exp(-\beta_{33,h}l^2)J_{-m}(2\pi l a_3), \quad (4.1)$$

(*b*) harmonic displacive modulation APC

$$|F^{APC}_{00lm}| = T^{APC}A^{APC} = \exp(-\beta_{33,0}l^2)\tilde{I}_{-m}(2\pi l a_3; -\beta_{33,0}l^2) \quad (4.2)$$

with

$$\tilde{I}_{-m}(2\pi l a_3; -\beta_{33,0}l^2) = \sum_{n=-\infty}^{\infty} J_{-m-2n}(2\pi l a_3) \times I_n(-\beta_{33,0}l^2) = \int_0^{2\pi} d\varphi \exp[2\pi i \sin(\varphi) - \beta_{33,0}l^2 \cos(2\varphi) + m\varphi] \quad (4.3)$$

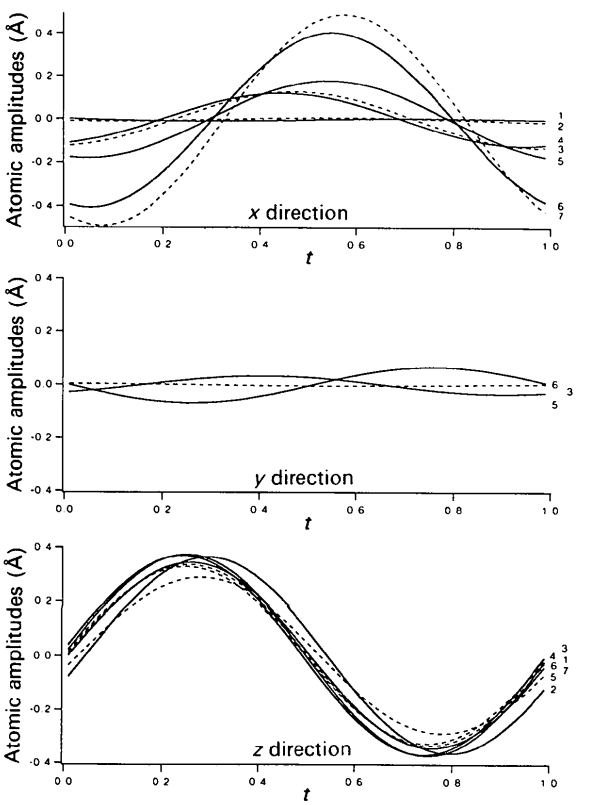

Fig. 3. Atomic modulation functions of model No. 5 in *x*, *y* and *z* directions. The numbers given on the right-hand side of the graphs refer to the following atoms: 1 Mn; 2 Cl1; 3 Cl2; 4 N; 5 C1; 6 C2; 7 C3.

where T is the thermal and A the positional part of the structure factor. The atom is placed at (0,0,0), the modulation phases are $\varphi_{3,1} = 0.75$ and $\chi_{33,2} = 0.00$ using expressions (3.7), (3.14) and (3.18). The reflections are limited to (00lm). These assumptions considerably simplify the structure factor as compared to the general expressions of Paciorek & Kucharczyk (1985). Expression (4.1) used the standard DWF for non-modulated structures while expression (4.2) employs the DWF of the APC theory as described by expressions (3.14)–(3.18). The phason contribution changes $\beta_{ij,h}$ to $\beta_{ij,0}$ [see (3.15)] in T and the cylindrical Bessel function J_{-m} to the Generalized Bessel function $\tilde{I}_{-m}$ in A. The relation (4.3) is taken from Paciorek & Chapuis (1994).

The expressions (4.1) and (4.2) are plotted in Fig. 5 using the modulation proportions of this structure. Each category of reflections shows it proper intensity enhancement and depletion behaviour. The intuitive guess that phasons/amplitudons decrease the intensity of all reflection categories is not necessarily true. As seen from (3.12) and (3.13), the Axe and Overhauser corrections play the role of additional scale factors for the satellite reflections. In favourable cases, these expressions can be sufficient to approximate case (*b*), especially since the interplay of scale factors, DWF and modulation amplitudes in the actual refinement could improve the fit. Obviously, a limited resolution both in $\sin\theta/\lambda$ and in satellite order reduces the chances of obtaining physically significant parameters from the refinement. This example illustrates the subtlety of the influence of the phasons on diffraction intensities.

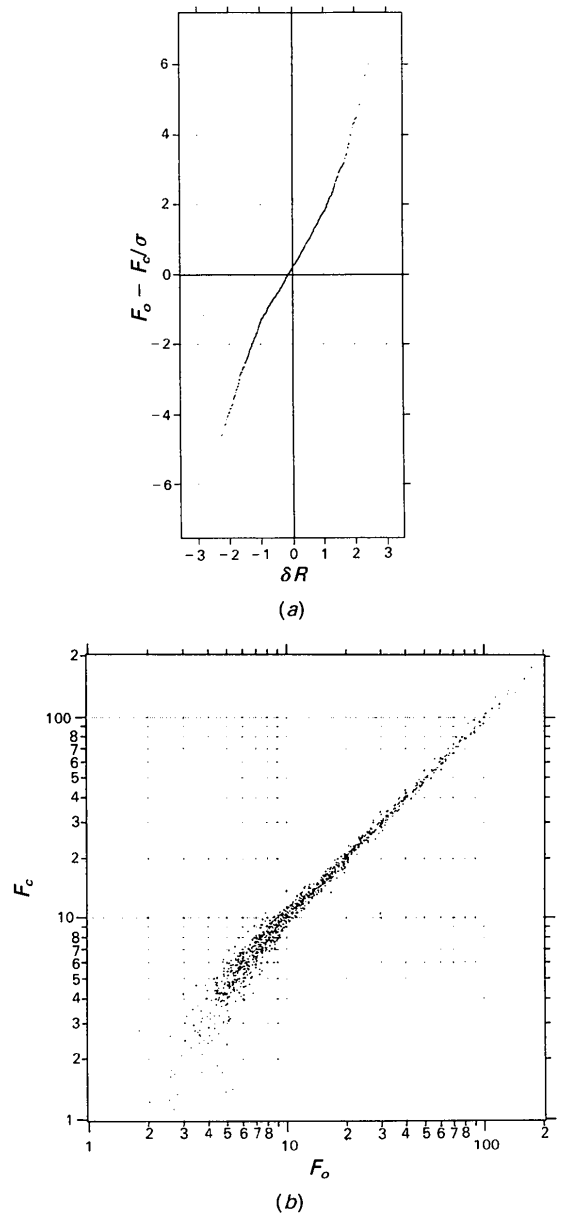

Fig. 4. (*a*) Normal probability plot and (*b*) F_c *vs* F_o plot for the reflection data of model No. 5.

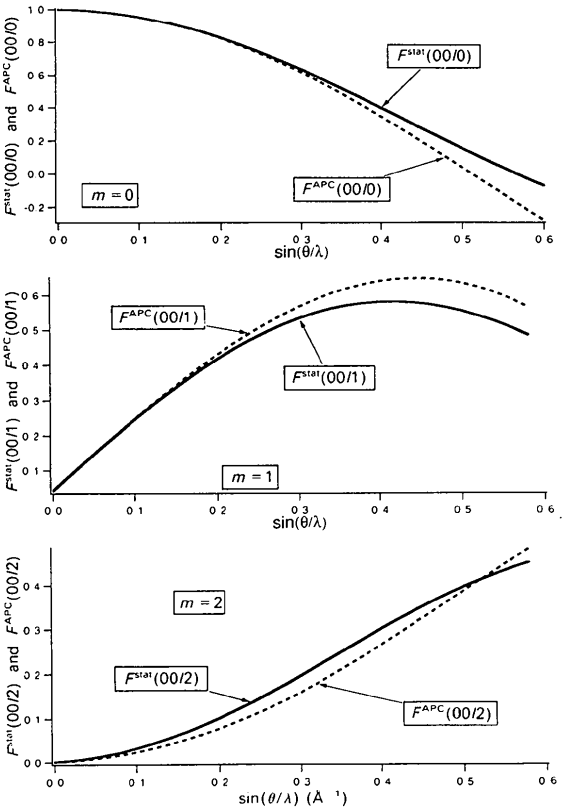

Fig. 5. Structure factors $|F^{stat}(00lm)|$ and $|F^{APC}(00lm)|$ of a monoatomic modulated Bravais lattice [parity 00lm with l continuous and $|m| \leq 2$; expressions (4.1) and (4.2)]. It should be noted that phasons (as parametrized by Pérez-Mato *et al.*, 1991) may deplete or *enhance* reflection intensities. Parameters used: $a_{3,1} = 0.0135$, $\beta_{33,2} = 0.0003$.

Table 7. *The modulated atomic Debye–Waller factors (model 6)*

Comparison of the refined values of positional modulation functions u_i^μ [see expression (3.7)] and the modulated atomic DWF β_{ij}^μ [see expression (3.14)] with the expected values $\varepsilon_{ij,2}$ (Pérez-Mato *et al.*, 1991) calculated in the following way

$$\varepsilon_{ij,2} = \varphi_{i,1} + \varphi_{j,1} + \pi.$$

In the expression below, +/− means phason/amplitudon dominance (see Fig. 1), symmetry constraints are indicated by * and arrows (←) pointing to values that deviate significantly from the predicted value $\varepsilon_{ij,2}u_i^\mu$ are multiplied by 10^4, and the DWF's by 10^3. The coordinates x_i of this model agree with those given in Table 5.

	a_1	a_2	a_3	$\beta_{11,0}$	$\beta_{22,0}$	$\beta_{33,0}$	$\beta_{12,0}$	$\beta_{13,0}$	$\beta_{23,0}$
	$\varphi_{1,1}$	$\varphi_{2,1}$	$\varphi_{3,1}$	$\beta_{11,2}$; $\chi_{11,2}$	$\beta_{22,2}$; $\chi_{22,2}$	$\beta_{33,2}$; $\chi_{33,2}$	$\beta_{12,2}$; $\chi_{12,2}$	$\beta_{13,2}$; $\chi_{13,2}$	$\beta_{23,2}$; $\chi_{23,2}$
				$\varepsilon_{11,2}$	$\varepsilon_{22,2}$	$\varepsilon_{33,2}$	$\varepsilon_{12,2}$	$\varepsilon_{13,2}$	$\varepsilon_{23,2}$
Mn	7 (1)	–	134.4 (8)	12.6 (4)	13.0 (3)	2.70 (4)	–*	0.12 (6)	–*
	0.25*	–	0.75*	1 (1); 0.00*	–	0.46 (6); 0.00*	–*	0.1 (2); 0.50*	–*
				0.00	–	0.00	–	0.50	–
Cl1	12 (2)	2 (3)	130.7 (9)	14.8 (4)	15.5 (5)	3.41 (4)	3.5 (2)	–*	–*
	0.00*	0.50*	0.25*	1 (1); 0.50*	−2 (1); 0.50*	0.55 (7); 0.00*	3 (1); 0.00*	2 (2); 0.75*	3 (3); 0.25*
				0.50	0.50	0.00	0.00	0.75	0.25
Cl2	167 (3)	–	132.3 (9)	21.6 (4)	30.4 (4)	2.76 (5)	–*	0.05 (9)	–*
	0.516 (3)	–	0.751 (1)	2 (1); 0.58 (8)	–	0.56 (7); 0.99 (2)	–*	1.0 (2); 0.79 (4)	–*
				0.532 (6)	–	0.002 (2)	–	0.767 (4)	–*
N	166 (9)	–	116 (3)	30 (1)	31 (2)	2.2 (1)	–*	0.00 (3)	–*
	0.461 (8)	–	0.253 (5)	−11 (5); 0.59 (6)	–	0.2 (3); 0.1 (2)	–*	0.5 (9); 0.0 (2)	*
				0.42 (2)←	–	0.01 (1)	–	0.21 (2)←	–
C1	260 (20)	130 (30)	112 (5)	61 (4)	30 (7)	3.1 (2)	10 (4)	−1.2 (8)	−1 (1)
	0.488 (9)	0.41 (3)	0.279 (8)	−37 (8); 0.29 (3)	−20 (11); 0.4 (1)	−0.8 (4); 0.09 (9)	−24 (9); 0.39 (7)	2 (1); 0.21 (5)	6 (2); 0.14 (5)
				0.48 (2)←	0.32 (6)	0.06 (1)	0.40 (4)	0.27 (2)	0.19 (4)
C2	640 (30)	130 (30)	130 (6)	109 (6)	39 (7)	3.3 (3)	−14 (5)	3 (1)	−1 (1)
	0.571 (5)	0.64 (4)	0.272 (9)	−60 (10); 0.68 (2)	−20 (10); 0.6 (1)	−0.9 (6); 0.08 (8)	−10 (10); 0.7 (1)	−8 (2); 0.49 (3)	−4 (2); 0.39 (9)
				0.61 (1)	0.8 (1)←	0.04 (2)	0.71 (5)	0.34 (1)←	0.41 (5)
C3	590 (20)	–	130 (6)	101 (5)	86 (5)	3.5 (3)	–*	4 (1)	–*
	0.566 (6)	–	0.224 (8)	20 (10); 0.51 (7)	–	1.5 (4); 0.20 (5)	–*	7 (2); 0.38 (4)	–*
				0.63 (1)	–	0.95 (2)←	–	0.29 (1)	–

Table 4 gives the agreement factors of the three phason-corrected harmonic models (4–6). The APC model (6) shows the best agreement on all reflection categories. The question arises whether the improvement of this elaborate model is significant in view of the 50 additional parameters when compared with the Axe or Overhauser correction. The Hamilton test (*International Tables for X-ray Crystallography*, 1974) indicates a significant improvement in applying the APC compared with the Overhauser and Axe correction at a 0.005 significance level.

Table 7 shows the refined values of the DWF, the modulation functions and the expected phase relation from (3.18). From the APC theory, positive amplitudes $\beta_{ij,2}$ can be expected, together with phases $\chi_{ij,2}$, satisfying condition (3.18). The amplitudes should be positive since the phason excitation [as described by $\langle\delta\varphi^2\rangle$ in expression (3.17)] requires a much lower energy than the amplitudon excitation [$\langle\delta\rho^2\rangle$ in (3.17)]. The octahedral atoms Mn, Cl1, Cl2 fulfill this expected behaviour. For Mn and Cl1 located on the special positions 4(*a*) and 8(*e*), the phases $\chi_{ij,2}$ are fixed by symmetry. The refinement of the $\beta_{ij,2}$'s yields the expected positive values. The special position of Cl2 allows refinement of the phases $\chi_{ij,2}$ with $ij = (11,33,13)$. The amplitudes and phases of the DWF modulation agree perfectly with the theoretical predictions. However, the atoms belonging to the propylammonium chain show a different behaviour. Most of the phases $\chi_{ij,2}$ agree with condition (3.18). The amplitudes $\beta_{ij,2}$ are, however, mostly negative, indicating an unexpected amplitudon dominance. It should be noted that in the incommensurate phase, the propylammonium chain has a large degree of orientational disorder which could explain the unexpected behaviour.

From the refined amplitudes $\beta_{ij,2}$, an estimate of $\langle\delta\varphi^2\rangle$ [see expression (3.17)] can be obtained. Under the assumption that $\langle\delta\varphi^2\rangle \gg \langle\delta\rho^2\rangle$, its value is about 0.3–0.4, which corresponds to a phase-fluctuation magnitude of about 30–40°. To the authors knowledge, no neutron data is available for comparison. However, the magnitude seems reasonable.

An illustration of the DWF modulation is shown in Fig. 6. Size and orientation of the probability ellipsoids vary as a function of the internal coordinate t.

The experimental findings support the APC theory, in a similar way to thiourea (Madariaga, Zuñiga, Paciorek, Ezpeleta & Etxebarria, 1990) and $ThBr_4$ (Madariaga *et al.*, 1993). The explicit use of expression (3.18) as a constraint on the DWF modulation phases $\chi_{ij,2}$ would reduce the number of parameters for the APC (model 6) from 51 to 29.

4.3. *Anharmonicity, first-harmonic DWF, hydrogens*

Three additional models were investigated in order to check if the phason effect might be an artifact due to the missing H atoms or the missing contributions to the displacive or DWF modulation wave (models 8, 3 and 7 in Table 4). None of the models were able to successfully accommodate main reflections, first- or second-order satellites. The second harmonics of the displacement amplitudes in model 3 were all negligible compared with the first harmonics. The amplitudes of the first-harmonic DWF modulation never exceeded one standard deviation and the refined phases show no correlation with the refined phases of the displacive modulation functions. The H atoms improved mainly the agreement of main reflections but had no influence on the second-order satellites. For all three models, a phason correction should be applied.

5. Concluding remarks

The general structural features revealed in this refinement agree with the description given by Depmeier (1981) in the commensurate approximation of the γ phase and with the Cd homologue of PAMC by Doudin & Chapuis (1990*a*). The modulation is harmonic displacive with amplitudes of about 0.3–0.4 Å in the *a* and *c* directions. The anharmonic contributions to the modulation are negligible. The refinement of the second harmonic of DWF is conclusive. The refined values for the octahedral atoms agree with the expectation from the amplitudon/phason correction theory. Inherent disorder and resolution limited to $\sin\theta/\lambda = 0.53$ Å^{-1} might explain the unexpected DWF modulation parameters of the propylammonium chain.

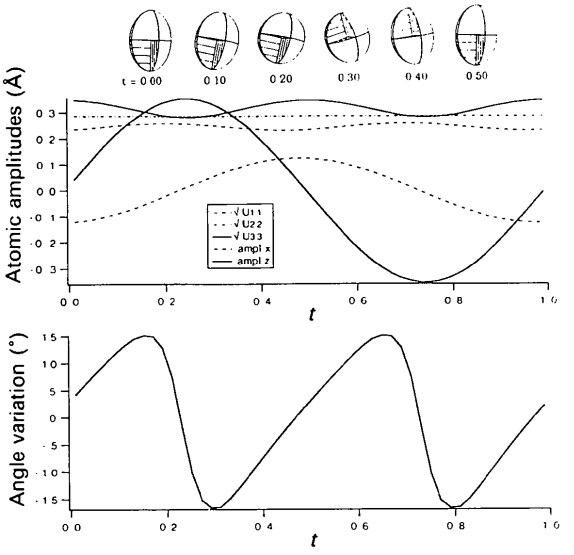

Fig. 6. Atomic modulation functions of Cl2 (model No. 6, upper graph). For this atom the positional parameters *x* and *z* are modulated (first harmonic) as well as the Debye–Waller terms U_{11}, U_{33} and U_{13} (second harmonic). For six values of *t* (internal coordinate), *ORTEP* (Johnson, 1965) plots of Cl2 are given (projection parallel to *b*) showing the rotation of the thermal ellipsoid as a function of *t* under Debye–Waller factor modulation. The lower graph shows the angle variation of one eigenvector of the thermal ellipsoid with respect to the *c* axis.

One of the authors (MM) is indebted to the DAAD (Deutscher Akademischer Austausch Dienst) and the Université de Lausanne for financial support. Financial support from the Swiss National Science Foundation is gratefully acknowledged. Comments from J. M. Pérez-Mato have been greatly appreciated.

References

Axe, J. D. (1980). *Phys. Rev. B*, **10**, 4181–4190.

Chapuis, G., Kind, R. & Arend, H. (1976). *Phys. Status Solidi A*, **36**, 285–295.

Depmeier, W. (1979). *J. Solid State Chem.* **29**, 15–26.

Depmeier, W. (1981). *Acta Cryst.* B**37**, 330–339.

Depmeier, W. (1983). *Solid State Commun.* **45**, 1089–1092.

Depmeier, W. (1986). *Ferroelectrics*, **66**, 109–123.

Depmeier, W. & Mason, S. A. (1978). *Acta Cryst.* B**34**, 920–922.

Doudin, B. & Chapuis, G. (1990*a*). *Acta Cryst.* B**46**, 175–180.

Doudin, B. & Chapuis, G. (1990*b*). *Acta Cryst.* B**46**, 180–186.

Holgervorst, A., Peterse, W. J. A. M. & de Wolff, P. M. (1979). *Proceedings of the International Conference on Modulated Structures*, edited by J. M. Cowley, J. B. Cohen, M. B. Salamon & B. J. Wuensch, pp. 217–219. New York: AIP.

Johnson, C. K. (1965). *ORTEP*. Report ORNL-3794. Oak Ridge National Laboratory, Tennessee, USA.

Lucken, A., Hagemann, H. & Bill, H. (1991). *J. Phys. Condens. Matter*, **3**, 5085–5097.

Madariaga, G., Pérez-Mato, J. M. & Aramburu, I. (1993). *Acta Cryst.* B**49**, 244–254.

Madariaga, G., Zuñiga, F. J., Paciorek, W. A., Ezpeleta, J. M. & Etxebarria, I. (1990). *Ferroelectrics*, **105**, 309–314.

Muralt, P. (1986). *J. Phys. C*, **19**, 1689–1704.

Muralt, P, Caravatti, P., Kind, R. & Roos, J. (1986). *J. Phys. C*, **19**, 1705–1719.

Overhauser, A. W. (1971). *Phys Rev. B*, **3**, 3173–3182.

Paciorek, W. A. (1991). *Methods of Structural Analysis of Modulated Structures and Quasicrystals*, edited by J. M. Pérez-Mato, F. J. Zúñiga & G. Madariaga, pp. 268–279. Singapore: World Scientific Publishing.

Paciorek, W. A. & Chapuis, G. (1994) *Acta Cryst.* A**50**, 194–203.

Paciorek, W. A. & Kucharczyk, D. (1985). *Acta Cryst.* A**41**, 462–466.

Pérez-Mato, J. M., Madariaga, G. & Elcoro, L. (1991). *Solid State Commun.* **78**, 33–37.

Peterson, E. R. & Willet, R. D. (1972). *J. Chem. Phys.* **56**, 1879–1882.

Rollet, J. S. (1965). In *Computing Methods in Crystallography*. Oxford: Pergamon Press.

Sheldrick, G. M. (1978). *SHELXTL. An Integrated System for Solving, Refining and Displaying Crystal Structures from Diffraction Data*. Univ. of Göttingen, Germany.

Steurer, W. & Depmeier, W. (1989). *Acta Cryst.* B**45**, 555–562.

Willis, B. T. M. & Pryor, A. W. (1975). In *Thermal Vibrations in Crystallography*. Cambridge Univ. Press.

Wolff, P. M. de (1974). *Acta Cryst.* A**30**, 777–785.

Wolff, P. M. de, Janssen, T. & Janner, A. (1981). *Acta Cryst.* A**37**, 625–636.

Yamamoto, A. (1982). *Acta Cryst.* A**38**, 87–92.